Nonlinear features of Northern Annular Mode variability

Zuntao Fu *, Liu Shi, Fenghua Xie, Lin Piao

Lab for Climate and Ocean-Atmosphere Studies, Department of Atmospheric and Oceanic Sciences, School of Physics, Peking University, Beijing, 100871, China

HIGHLIGHTS

- Nonlinear features of daily NAM variability are quantified.
- Two measures reach the same conclusion.
- Nonlinear features in NAM variation are significant at lower pressure levels.

ARTICLE INFO

ABSTRACT

Nonlinear features of daily Northern Annular Mode (NAM) variability at 17 pressure levels are quantified by two different measures. One is nonlinear correlation, and the other is time-irreversible symmetry. Both measures show that there are no significant nonlinear features in NAM variability at the higher pressure levels, however as the pressure level decreases, the strength of nonlinear features in NAM variability becomes predominant. This indicates that in order to reach better prediction of NAM variability in the lower pressure levels, nonlinear features must be taken into consideration to build suitable models.

© 2016 Elsevier B.V. All rights reserved.

1. Introduction

The North Atlantic Oscillation (NAO)/ Arctic Oscillation (AO) is the dominant pattern of climate variability affecting North Atlantic region and western Europe [1]. The pattern mentioned above also has been taken as the near-surface Northern Annular Mode (NAM) [2–4], since NAM has been defined separately at each isobaric level from Earth's surface through the stratosphere [2]. NAM contains a broad spectrum of variations [5], however fundamental mechanisms determining the evolution of NAM are still far from being elucidated over each scale. For example, previous studies have found out that NAO index possesses distinct behaviors over a range of timescales and there is no one process that can likely account for all variabilities [1,5,6]. It has been suggested that the yearly NAO index is a stationary process with long-range correlation rather than a non-stationary random walk [5], although there are structured components, they can only explain less than 15% of the variations in the NAO index itself [7]. And that is why some scientists have obtained bad predictive performance when using pink noise as a model of yearly NAO index [8,9]. Furthermore, the dynamics of NAO is also associated with intra-seasonal time scales, which leads to the results that the daily NAM(NAO) index exhibits distinct behaviors from the yearly data [1,6,10,11]. Predominant nonlinear features are found in daily NAM (NAO) index: (i) Auto-regressive models fail to describe the daily NAM index at 1000 hPa and the spectra of daily NAM index are more consistent with low-order chaos [6], (ii) The duration of NAO pattern is extremely different over different phases [10].

According to the studies above, we find that the strength of nonlinear features may change for 1000 hPa NAM variability on the different time scales. However it is not clear whether the strength of nonlinear features in NAM variability is different

---

at different pressure levels for a given time scale range. As we all know, the stratospheric harbingers may be a superior predictor of tropospheric weather regimes [2–4], therefore better understanding of nonlinear feature of NAM variability at different pressure levels is really necessary because only in this way we can build more suitable statistical model and make skillful climate prediction.

The nonlinear features of NAM index series can be quantified by two different kinds of approaches. Firstly, nonlinearity could result in an asymmetry of certain statistical properties under time reversal, therefore temporal irreversibility of time series is an important indirect quantitative assessment of nonlinearity [12,13]. A stationary process $x(t)$ is said to be time reversible if for every n, the series $\{x_1, \ldots, x_n\}$ and $\{x_n, \ldots, x_1\}$ have the same joint probability distributions [14]. More importantly, we need to address that quantifying the nonlinearity by means of time irreversibility has been widely applied to study nonlinear features in observational time series from various fields, such as physiology [15–18]. What is more, several statistical tests have been developed toward detection and quantification of irreversibility in time series [16–20]. Most recently, Lacasa and his colleges developed a method [19] based on horizontal visibility graph [21], which is an algorithmic variant of visibility graphs [22]. Without extra amount of ad hoc information for symbolization procedure, they show that irreversible dynamics results in an asymmetry between the probability distributions of the numbers of incoming and outgoing links in directed horizontal visibility graphs (DHVG) of given time series [18,19]. Therefore, in this paper we will characterize the nonlinear features of NAM variability at each pressure level through time series irreversibility by using the DHVG method. Secondly, nonlinear feature can be quantified by the nonlinear correlation, where original series x_i will be decomposed into magnitude series $|\triangle x_i| \equiv |x_{i+1} - x_i|$. If long-range correlation is found in the magnitude series $|\triangle x_i|$, and then this means the underlying process possesses the characteristics of nonlinearity [23–27]. Thus, here we will use detrended fluctuation analysis (DFA) [28,29] to quantify the strength of long-range correlation in time series. If the root mean square fluctuation function, $F(s)$, is proportional to s^α, where s is the window scale, the series is long range correlated. For a random series, $\alpha = 0.5$, while for long-range correlated series, $\alpha > 0.5$.

The rest of the paper is organized as follows. In Section 2, we will make a brief introduction to the data sets used in this paper. The results will be discussed in Section 3. In Section 4, discussions and conclusions are made.

2. Data

The data used in this study are daily and monthly mean temperatures and geo-potential height fields of the period of 1948–2010 from 1000 hPa to 10 hPa. The data are downloaded from National Centers for Environmental Prediction-National Center for Atmospheric Research(NCEP/NCAR) reanalysis project and are applied to calculate NAM index just like what Baldwin et al. have done [2]. Next, we calculate the climatological annual cycle of the NAM index as the average of the same of each year at each latitude, longitude, pressure level. And then this annual cycle is subtracted to obtain anomalies from 20 °N to the North Pole. The wintertime (December–February) monthly mean data are used to calculate the leading Empirical Orthogonal Function (EOF) spatial pattern [10]. Here a separate EOF is made for each pressure level. Daily values of the NAM, spanning over the entire 63-year data record, are calculated for each pressure level by projecting daily geo-potential anomalies onto the leading EOF patterns. In order to compare the features of daily NAM index at the 17 pressure levels, we normalize the NAM index on each level by subtracting its mean value and dividing standard deviation over the whole span. Four typical daily normalized NAM indices over four pressure levels are presented in Fig. 1(a), where we can see there are marked different behaviors in NAM variations over the different pressure levels. In order to remove the non-stationary variations of NAM index at the lower pressure levels during the cold seasons, day-to-day difference in NAM index $\triangle NAM_i = NAM_{i+1} - NAM_i$ is chosen to be analyzed. The nonlinear correlation can be estimated from the normalized variable $|\triangle NAM|$, where its seasonal cycle has been subtracted and its standard deviation has been divided. Four typical normalized $|\triangle NAM|$ indices at four pressure levels are presented in Fig. 1(b), where we can see that the marked variations at the lower pressure levels during the cold seasons have been nearly eliminated and the behaviors on both higher and lower pressure levels are close to each other.

3. Results

3.1. DFA results

First of all, we analyze the normalized NAM and $|\triangle NAM|$ index series to learn about the long-range correlation and nonlinear correlation hidden in the variations of NAM index. Due to non-overlapping annual cycle for each year in the NAM variation, we cannot totally eliminate the effect of the annual cycle in the normalized NAM index by the usual normalized procedure. From the DFA results for NAM index at each pressure level, we cannot find a scaling range extending far enough to estimate the long-range correlation exponent α. The lower the pressure level is, the more predominant cross-over in scaling range, see Fig. 2(a). Since the long-range correlation of NAM variation is not the focus of this paper, we will not give further analysis on it. However, different from DFA result of NAM variations, extended scaling ranges are found for $|\triangle NAM|$ variations at each pressure level, see Fig. 2(b). Furthermore, in order to compare the DFA results from different pressure levels, we estimate the DFA scaling exponent $\alpha_{|\triangle NAM|}$ on each pressure level from 10 days to 1.5 years, which is also the range connecting NAM variations from higher frequencies to lower frequencies. And most important, the DFA scaling exponent, $\alpha_{|\triangle NAM|}$, is not constant for all 17 pressure levels, at the higher pressure levels, $\alpha_{|\triangle NAM|}$ is close to 0.5, which indicates there
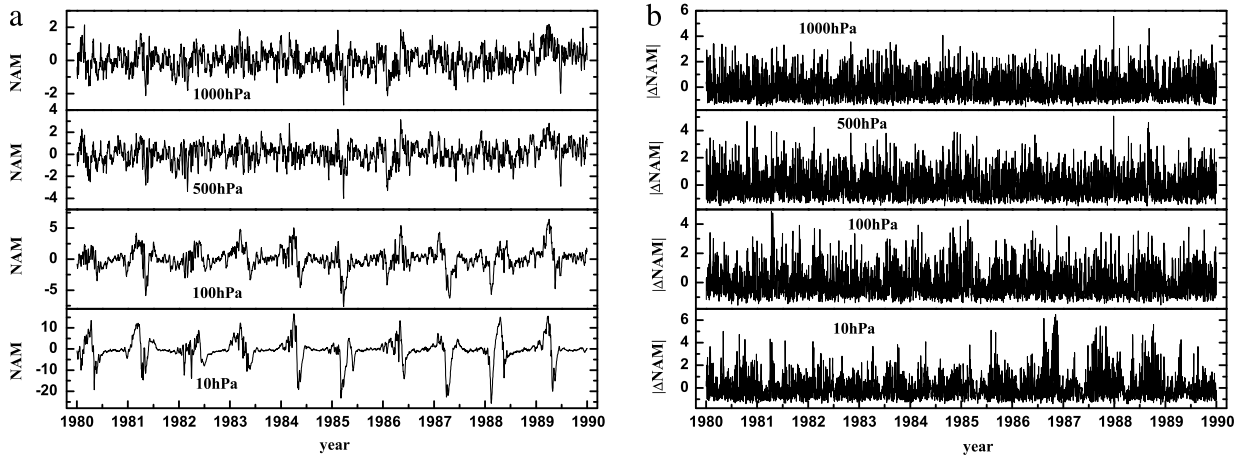
Fig. 1. Typical series over four pressure levels, 1000 hPa, 500 hPa, 100 hPa and 10 hPa from (a) NAM and (b) normalized |△NAM|.
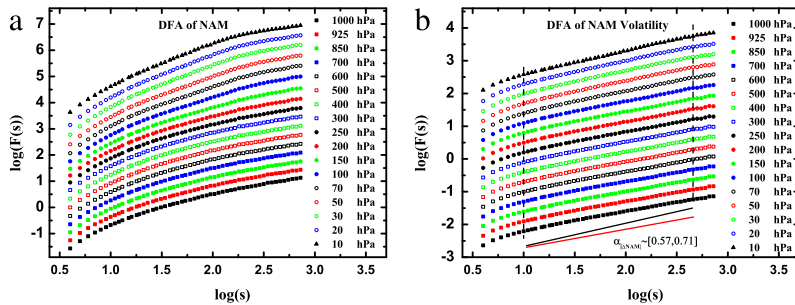
Fig. 2. DFA results for (a) NAM and (b) |△NAM| over 17 pressure levels, where red solid line with slope of 0.5 denotes the case for without correlation and the black solid line with slope of 0.71 denotes the case for the maximal correlation in NAM variations on all 17 pressure levels. It should be noted that the fitted scaling ranges for $\alpha_{|\triangle NAM|}$ are chosen from 10 days to 1.5 years.

is no nonlinear correlation; however, with the pressure level decreasing, the value of $\alpha_{|\triangle NAM|}$ is increasing, the largest value of $\alpha_{|\triangle NAM|}$ is close to 0.71, see Fig. 3, which is greatly deviated from 0.5 and indicates there is marked nonlinear correlation in NAM variations at the lower pressure levels. Using the surrogating procedure [30,31], we can generate 1000 samples of surrogate data from the linear processes of the same data length as these of NAM index used in this paper to calculate 1000 $\alpha_{|\triangle NAM|}$, here we choose the maximum value of $\alpha_{|\triangle NAM|}$ from the 1000 surrogate data as the critical threshold, which is shown in Fig. 3 as the dot line. If the $\alpha_{|\triangle NAM|}$ for |△NAM| variations on specific pressure level are larger than this critical threshold, the NAM variation on this pressure level is considered to take nonlinear correlation feature. We can see that all the values of $\alpha_{|\triangle NAM|}$ on the pressure levels smaller than 200 hPa are larger than this critical threshold, so we can say there are marked nonlinear correlations in NAM variation from the pressure levels smaller than 200 hPa (including 200 hPa), here the critical pressure level is 250 hPa.

3.2. DHVG results

The general purpose of visibility algorithm is to accurately map the information stored in a time series into an alternative mathematical structure, thus graph theory can be employed to study nonlinear feature hidden in the nonlinear time series [19]. The directed graph was first introduced by Lacasa and his colleagues [19] by defining a DHVG, where the degree $k(t)$ of node t is now split into an ingoing degree $k_{in}(t)$, and an outgoing degree $k_{out}(t)$, such that $k(t) = k_{in}(t) + k_{out}(t)$. The ingoing degree $k_{in}(t)$ is defined as the number of links of node t with other past nodes associated with data in the series (that is, nodes with $t' < t$). The outgoing degree $k_{out}(t)$ is defined as the number of links with future nodes (that is, nodes with $t' > t$). The in and out degree distributions of a DHVG are defined as the probability distributions of $k_{out}(t)$ and $k_{in}(t)$ of the graph, where $p_{out}(k) \equiv p(k_{out} = k)$ and $p_{in}(k) \equiv p(k_{in} = k)$.

The information stored in the *in* and *out* distributions can be taken into account for the amount of time irreversibility of the associated series. And this can be measured as the distance (in a distributional sense) between the *in* and *out* degree distributions [32],

$$L(p_{in}\|p_{out}) = \sum_k |p_{in}(k) \log p_{in}(k) - p_{out}(k) \log p_{out}(k)|. \tag{1}$$
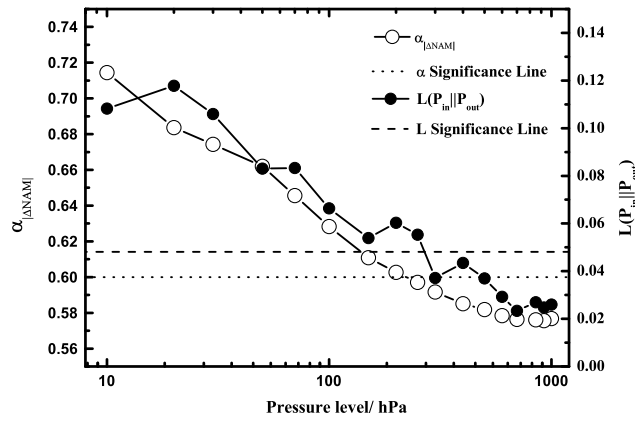
Fig. 3. Variation of $\alpha_{|\triangle NAM|}$ and $L(P_{in}\|P_{out})$ with height, where horizontal dash and dot lines are critical threshold for $L(P_{in}\|P_{out})$ and $\alpha_{|\triangle NAM|}$, respectively.
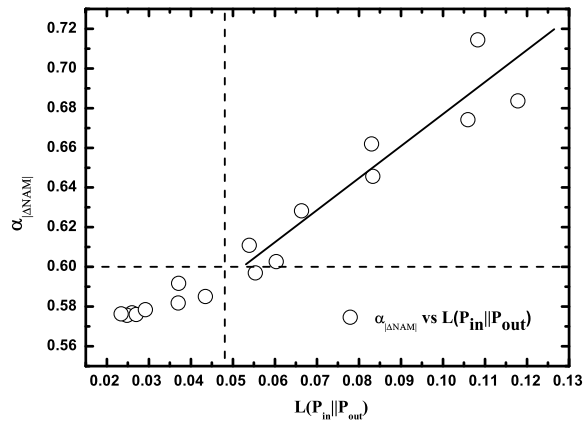
Fig. 4. Scatter plot of $\alpha_{|\triangle NAM|}$ v.s. $L(P_{in}\|P_{out})$, where the vertical and horizontal dash lines are critical threshold for $L(P_{in}\|P_{out})$ and $\alpha_{|\triangle NAM|}$, respectively.

We apply the DHVG method to the normalized NAM index at each pressure level to calculate the ingoing degree $k_{in}(t)$ and outgoing degree $k_{out}(t)$ and we can use these results and the measure (1) to quantify strength of the nonlinear features hidden in the NAM variations, detailed results are presented in Fig. 3. Here we can see that the value of this measure $L(p_{in}\|p_{out})$ increases with the pressure level decreasing. At the same time, we can see that this property is similar to those of nonlinear correlation quantified by $\alpha_{|\triangle NAM|}$, with the pressure level decreasing, both measures $L(p_{in}\|p_{out})$ and $\alpha_{|\triangle NAM|}$ nearly increase monotonically, where the variation of $\alpha_{|\triangle NAM|}$ is much smoother, while the variation of $L(p_{in}\|p_{out})$ takes a little fluctuation. If the measure $L(p_{in}\|p_{out})$ is smaller than a critical threshold, then it can be inferred the underlying process is a linear process. This threshold can be calculated from the 1000 surrogate data generated from linear processes, similarly, we choose the maximum value of $L(p_{in}\|p_{out})$ from 1000 surrogate data as the critical threshold, which is dash line given in Fig. 3. Although the critical values of both measures are different, they give nearly the same critical pressure level, from the measure $L(p_{in}\|p_{out})$, the critical pressure level is 300 hPa. For pressure levels smaller than 250 hPa (including 250 hPa), the NAM variations take the feature of time irreversibility, which is a kind of nonlinear behavior.

4. Conclusion and discussion

From above analysis, we can say that there are different nonlinear features in the NAM variations at the higher and lower pressure levels. Both measures $\alpha_{|\triangle NAM|}$ and $L(p_{in}\|p_{out})$ show that there are marked nonlinear features in NAM variations at pressure levels smaller than certain critical value, say 200 or 250 hPa. Actually, there is a great well one-to-one correspondence between $\alpha_{|\triangle NAM|}$ and $L(p_{in}\|p_{out})$, see Fig. 4. Above the critical pressure threshold, $\alpha_{|\triangle NAM|}$ nearly does not vary with $L(p_{in}\|p_{out})$, especially for the highest pressure levels. However, below a certain specific pressure level, $\alpha_{|\triangle NAM|}$ nearly changes linearly with $L(p_{in}\|p_{out})$, which mostly occurs in the lowest pressure levels. So both measures reach the same conclusion that nonlinear variations in NAM variation at the lower pressure levels cannot be omitted, whereas the NAM variation at the higher pressure levels can be taken to be from the linear processes, this is in line with the previous results reported on NAO variations [5,8,7,9]. In order to make better prediction on the variations at lower pressure levels, the best model must be chosen to incorporate nonlinear features found in the NAM variations at lower pressure levels,

since stratospheric harbingers can be taken as a predictor of tropospheric weather regimes [2–4]. How to incorporate the nonlinear feature to build models to fit the NAM variation at lower pressure levels best deserves further studies.

From our studies, we cannot say whether there is any clue of chaotic properties in NAM variations, though it has been argued variation of Arctic Oscillation index for higher frequencies is nonlinear with determinism beyond pseudo-periodicity [11], 1000 hPa NAM cannot be described by autoregressive models for higher frequencies and their spectra are more consistent with low-order chaos [6]. The nonlinear features found in NAM variations at lower pressure levels deserve further studies along this direction.

Acknowledgments

References

[1] S.P.E. Keeley, R.T. Sutton, L.C. Shaffrey, Does the North Atlantic Oscillation show unusual persistence on intraseasonal timescales? Geophys. Res. Lett. 36 (2009) L22706.
[2] M.P. Baldwin, T.J. Dunkerton, Stratospheric harbingers of anomalous weather regimes, Science 294 (2001) 581–584.
[3] M.P. Baldwin, D.B. Stephenson, D.W.J. Thompson, T.J. Dunkerton, A.J. Charlton, A. O'Neill, Stratospheric memory and skill of extended-range weather forecasts, Science 301 (2003) 636–640.
[4] M.P. Baldwin, D.W.J. Thompson, E.F. Shuckburgh, W.A. Norton, P.G. Nathan, Weather from the stratosphere, Science 301 (2003) 317–318.
[5] D.B. Stephenson, V. Pavan, R. Bojariu, Is the North Atlantic Oscillation a random walk?, Int. J. Climatol. 20 (2000) 1–18.
[6] S.M. Osprey, M.H.P. Ambaum, Evidence for the chaotic origin of Northern Annular Mode variability, Geophys. Res. Lett. 38 (2011) L15702.
[7] T.C. Mills, Is the North Atlantic Oscillation a random walk? A comment with further results, Int. J. Climatol. 24 (2004) 377–383.
[8] I. Fernandez, N. Carmen, N. Hernandez, J.M. Pacheco, Is the North Atlantic Oscillation just a pink noise? Phys. A 322 (2003) 705–714.
[9] I. Fernandez, J.M. Pacheco, M.P. Quintana, Pinkness of the North Atlantic Oscillation signal revisited, Phys. A 389 (2010) 5801–5807.
[10] S. Blessing, K. Fraedrich, M. Junge, T. Kunz, F. Lunkeit, Daily North-Atlantic Oscillation (NAO) index: Statistics and its stratospheric polar vortex dependence, Meteorol. Z. 14 (2005) 763–769.
[11] Y. Hirata, Y. Shimo, H.L. Tanaka, K. Aihara, Chaotic properties of the arctic oscillation jndex, SOLA 7 (2011) 33–36.
[12] C. Diks, J.C. van Houwelingen, F. Takens, J. DeGoede, Reversibility as a criterion for discriminating time series, Phys. Lett. A 201 (1995) 221–228.
[13] L. Stone, G. Landan, R.M. May, Detecting time's arrow: A method for identifying nonlinearity and deterministic chaos in time-series data, Proc. R. Soc. Lond. B 263 (1996) 1509–1513.
[14] G. Weiss, Time-reversibility of linear stochastic processes, J. Appl. Probab. 12 (1975) 831–836.
[15] M. Costa, A.L. Goldberger, C.K. Peng, Broken asymmetry of the human heartbeat: Loss of time irreversibility in aging and disease, Phys. Rev. Lett. 95 (2005).
[16] C. Cammarota, E. Rogora, Time reversal, symbolic series and irreversibility of human heartbeat, Chao Solitons Fractals 32 (2006) 1649–1654.
[17] M. Costa, C.K. Peng, A.L. Goldberger, Multiscale analysis of heart rate dynamics: entropy and time irreversibility measures, Cardiovasc. Eng. (2008) http://dx.doi.org/10.1007/s10558-007-9049-1.
[18] J.F. Donges, R.V. Donner, J. Kurths, Testing time series irreversibility using complex network methods, EPL 102 (2013) 10004.
[19] L. Lacasa, A. Nuñez, E. Roldan, J.M.R. Parrondo, B. Luque, Time series irreversibility: A visibility graph approach, Eur. Phys. J. B 85 (2012) 217.
[20] C.S. Daw, C.E.A. Finney, M.B. Kennel, Symbolic approach for measuring temporal irrevetsibility, Phys. Rev. E 62 (2000) 1912–1921.
[21] B. Luque, L. Lacasa, F. Ballesteros, J. Luque, Horizontal visibility graphs: Exact results for random time series, Phys. Rev. E 80 (2009).
[22] L. Lacasa, B. Luque, F. Ballesteros, J. Luque, J.C. Nuño, From time series to complex networks: The visibility graph, Proc. Natl. Acad. Sci. 105 (2008) 4972–4975.
[23] Y. Ashkenazy, P.Ch. Ivanov, S. Havlin, C.K. Peng, A.L. Goldberger, H.E. Stanley, Magnitude and sign correlations in heartbeat fluctuations, Phys. Rev. Lett. 86 (2001) 1900–1903.
[24] Y. Ashkenazy, S. Havlin, P.C. Ivanov, C.K. Peng, V. Schulte-Frohlinde, H.E. Stanley, Magnitude and sign scaling in power-law correlated time series, Physica A 323 (2003) 19–41.
[25] Y. Ashkenazy, D.R. Baker, H. Gildor, S. Havlin, Nonlinearity and multifractality of climate change in the past 420,000 years, Geophys. Res. Lett. 30 (2003) 2146.
[26] T. Kalisky, Y. Ashkenazy, S. Havlin, Volatility of linear and nonlinear time series, Phys. Rev. E 72 (2005).
[27] F.Y. Lu, N.M. Yuan, Z.T. Fu, J.Y. Mao, Universal scaling behaviors of meteorological variables' volatility and relations with original records, Phys. A 391 (2012) 4953–4962.
[28] C.K. Peng, S.V. Buldyrev, S. Havlin, M. Simons, H.E. Stanley, A.L. Goldberger, Mosaic organization of DNA nucleotides, Phys. Rev. E 49 (1994) 1685–1689.
[29] J.W. Kantelhardt, E. Koscielny-Bunde, H.H.A. Rego, S. Havlin, A. Bunde, Detecting long-range correlations with detrended fluctuation analysis, Physica A 295 (2001) 441–454.
[30] T. Schreiber, A. Schmitz, Improved surrogate data for nonlinearity tests, Phys. Rev. Lett. 77 (1996) 635–638.
[31] H.A. Makse, S. Havlin, M. Schwartz, H.E. Stanley, Method for generating long-range correlations for large systems, Phys. Rev. E 53 (1996) 5445.
[32] F.H. Xie, Z.T. Fu, L. Piao, J.Y. Mao, Time irreversibility of mean temperature anomaly variations over China, Theor. Appl. Climatol. (2015) http://dx.doi.org/10.1007/s00704-014-1347-0.